

*Letter to the Editor***The strange mid-infrared spectrum of M 31: ISOCAM observations***D. Cesarsky¹, J. Lequeux², L. Pagani², C. Ryter³, L. Loinard⁴, and M. Sauvage³¹ Institut d'Astrophysique Spatiale, Bat. 121, Université Paris XI, F-91450 Orsay Cedex, France² DEMIRM, Observatoire de Paris, 61 Avenue de l'Observatoire, F-75014 Paris, France³ SAp/DAPNIA/DSM, CEA-Saclay, F-91191 Gif sur Yvette Cedex, France⁴ IRAM, 300 Rue de la Piscine, Domaine Universitaire, F-38406 St Martin d'Hères Cedex, France

Received 10 June 1998 / Accepted 3 August 1998

Abstract. We present observations of the mid-IR spectrum of 4 small regions of M 31. The spectrum of the central 3' is characterized by a strong, broad unidentified emission band (UIB) at 11.3 μm while the other usual UIBs at 6.2, 7.7 and 8.6 μm are absent or very faint. We present a map of this area in the 11.3 μm band and compare it with optical and H I images. The spectra of two other regions are similar; one of these regions is in the bulge, and the other one in a quiet region of the star-forming ring at 10 kpc radius. The spectrum of a more active region of this ring shows relatively stronger 6.2, 7.7 and 8.6 μm bands. The profile of the 11.3 μm band varies from field to field. We suggest that we see in M 31 the emission of hydrogenated amorphous carbon particles as synthesized in the atmospheres of carbon stars. These particles have mid-infrared emission or absorption bands at 3.3–3.4 μm and 11.3 μm only. They have to be graphitized by UV radiation to be able to emit the other UIBs. This can take place in planetary nebulae, but most particles escape this processing, and are only affected by the interstellar UV field. The interstellar radiation field in M 31 is exceptionally poor in UV, e.g. compared to that in the solar neighbourhood. It is insufficient to graphitize the particles, hence the faintness of the 6.2, 7.7 and 8.6 μm UIBs.

Key words: galaxies: M 31 – galaxies: ISM – dust, extinction – infrared: ISM: lines and bands – infrared: stars – stars: carbon

1. Introduction

The Andromeda galaxy M 31 differs from our Galaxy in a number of ways. The most important for our purpose is the presence of a very large inner region essentially devoid of star formation. Most of the star formation is concentrated in a ring 10 kpc in

Send offprint requests to: james.lequeux@obspm.fr

* Based on observations with ISO, an ESA project with instruments funded by ESA member states (especially the PI countries: France, Germany, the Netherlands and the United Kingdom) and with the participation of ISAS and NASA.

radius, but even there the rate of star formation per unit area is modest. The luminosity in the central regions is dominated by the big stellar bulge, with very little ultra-violet emission except in the central few minutes. Still, these regions contain interstellar matter seen through a weak 21-cm (e.g. Brinks & Shane 1984) and CO line emission (Loinard et al. 1995), through far-IR emission (Xu & Helou 1996), as dust absorption patches projected over the light of the bulge and the disk (Hodge 1980) and finally through emission from ionized gas (e.g. Boulesteix et al. 1987).

Because of these differences, we decided to observe the mid-IR emission of characteristic regions of M 31 with the Infrared Space Observatory (ISO). Observations have been made in the open time and in the supplementary guaranteed time with the Circular Variable Filters of the ISOCAM camera in four regions of M 31, 3' \times 3' each. We report here the results of these observations, which are completely unexpected. Observations of more extended areas with broad- and narrow-band ISOCAM filters are described and analyzed by Lequeux et al. (1998).

2. Observations and data reduction

The observations have been made with the 32 \times 32 element mid-infrared camera (CAM) on board of the ISO satellite, with the Circular Variable Filters (CVFs) (see Cesarsky et al. 1996a for a complete description). The observations employed the 6'' per pixel field-of-view of CAM. Full scans of the two CVFs in the long-wave channel of the camera have been performed in the direction of decreasing or increasing wavelength according to the field. The total wavelength range covered is 5.15 to 16.5 μm . 10 \times 2.1s exposures were added for each step of the CVF, and 20 extra exposures were added at the beginning of each scan in order to limit the effect of the transient response of the detectors. The total observing time was about 1 hour per field. For the quiet region in the ring (whose spectrum is displayed in Fig. 3d) we made two CVF scans and the observing time was about 2 hours. The raw data were processed as described in Cesarsky

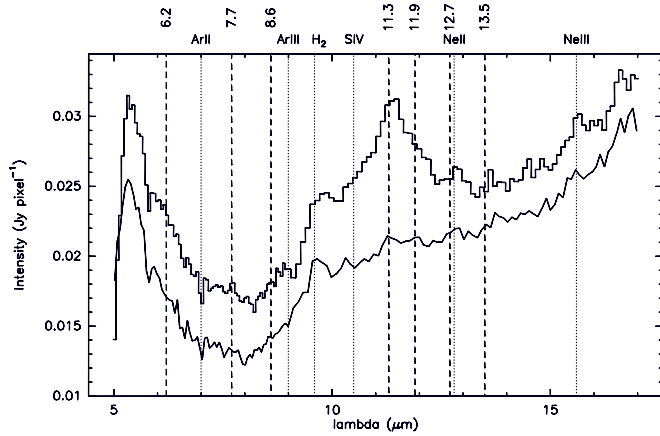


Fig. 1. Raw spectra from the center of M 31. The histogram-like spectrum represents the mean of the 35 pixels above $1.65 \times 10^{-16} \text{ W m}^{-2}$ per $6'' \times 6''$ pixel in the map of Fig. 2; the continuous spectrum represents the mean of the 79 pixels below $2.35 \times 10^{-17} \text{ W m}^{-2}$ per $6'' \times 6''$ pixel. The wavelengths of the usual emission lines (dotted lines) and bands (dashed lines) are indicated. The offset between the two is mostly due to uneven zodiacal light contamination because of light reflection and scattering inside the camera. The flux scale uncertainty is 30%

et al. (1996b) using the CIA software¹ (Biviano et al. 1997; Abergel et al. 1998; Starck et al. 1998).

The signals from the galaxy are everywhere faint with respect to the zodiacal emission which dominates the observed spectra. This emission cannot be measured or estimated with sufficient accuracy to allow proper subtraction. In consequence, we computed differential spectra between regions of relatively strong and weak emission, after averaging over the corresponding pixels (Fig. 1): as we can see in this figure, the $11.3 \mu\text{m}$ Unidentified Emission Band (UIB) is sufficiently strong to be mapped. By applying two thresholds to these maps, we defined the regions of strong and weak emission from which we computed the differential spectra. The thresholds gave between 35 and 260 pixels. This averaging alleviates the problem of spurious features due to cosmic ray impacts, which are limited to a few pixels. We checked that the differential spectra were only weakly dependant upon the actual threshold level. Variations of $\pm 50\%$ in the threshold level resulted in much smaller variations upon the baseline (typically 10%). These spectra are not completely free of zodiacal emission because of scattered and reflected light inside the camera. This explains most of the offset between the two spectra of Fig. 1 and thus the continuum emission, if any, cannot be determined. Fortunately the zodiacal spectrum is very smooth (Reach et al. 1996) and the narrow spectral features stand out unaffected. Finally, we had to subtract a baseline from the differential spectra. The flux level uncertainty is 30% at this stage.

¹ CIA is a joint development by the ESA Astrophysics Division and the ISOCAM Consortium led by the ISOCAM PI, C. Cesarsky, Direction des Sciences de la Matière, C.E.A., France

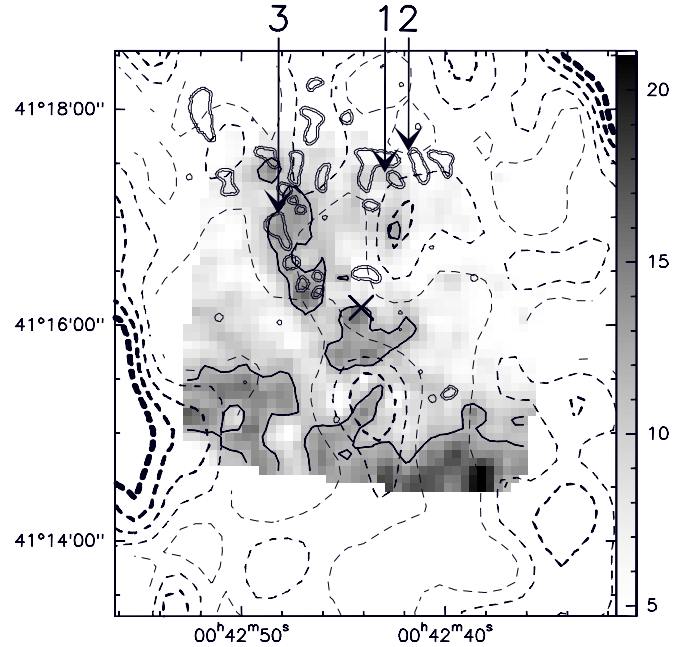


Fig. 2. Map of the center of M 31 in the $11.3 \mu\text{m}$ emission band (grey scale, with intensities in units of $10^{-17} \text{ W m}^{-2}$ per $6'' \times 6''$ pixel, a thick line delineates the level at 12 units). Coordinates are J2000, and the nucleus of the galaxy is at $\alpha = 00^{\text{h}}42^{\text{m}}44.10^{\text{s}}$, $\delta = 41^{\circ}16'09.9''$ (indicated by a cross). The contours of optical absorption (dust clouds) from Hodge (1980) are indicated by a double line, stars by a single thin line and those of the distribution of H I (Brinks & Shane 1984) by dotted lines whose thickness increases with intensity: levels 75 to 275 by steps of 50 K km s^{-1} . Some H I emission might come from the warp behind the disk. The positions towards which CO (1-0) line emission has been sought but not found by Loinard et al. (1996a) are indicated by the tips of the arrows: the $1-\sigma$ limit in 10.4 km s^{-1} channels is 12 mK for position 1 and 24 mK for positions 2 and 3.

3. Results

3.1. The $11.3 \mu\text{m}$ map of the center of M 31

Fig. 2 contains a map of the central $3' \times 3'$ of M 31 in the $11.3 \mu\text{m}$ band. This map has been re-centered on the nucleus which is well visible in the continuum at $5\text{--}6 \mu\text{m}$. The intensity range goes from -3.4×10^{-17} to $25.7 \times 10^{-17} \text{ W m}^{-2}$ per $6'' \times 6''$ pixel. Pixels below $7 \times 10^{-17} \text{ W m}^{-2}$ per $6'' \times 6''$ pixel are blanked out. This represents twice the rms fluctuation between five different map constructions. Above this threshold, we believe the features to be real. Due to the uncertain baseline subtraction, the flux scale precision is no better than 50%. Over this map the contours of the dark clouds from Hodge (1980) are superimposed. The correspondance is fair in the upper part. Faint absorption marks are seen at the position of the strong $11.3 \mu\text{m}$ emission to the south in Fig. 1 of Johnson & Hanna (1972). It is clear that the visibility of dust clouds depends very much on the stellar background. Fig. 2 also contains low-resolution ($24'' \times 36''$) contours of the distribution of the atomic gas from Brinks & Shane (1984). We note that Loinard et al. (1996a) have observed, but not detected CO with the IRAM 30-m telescope

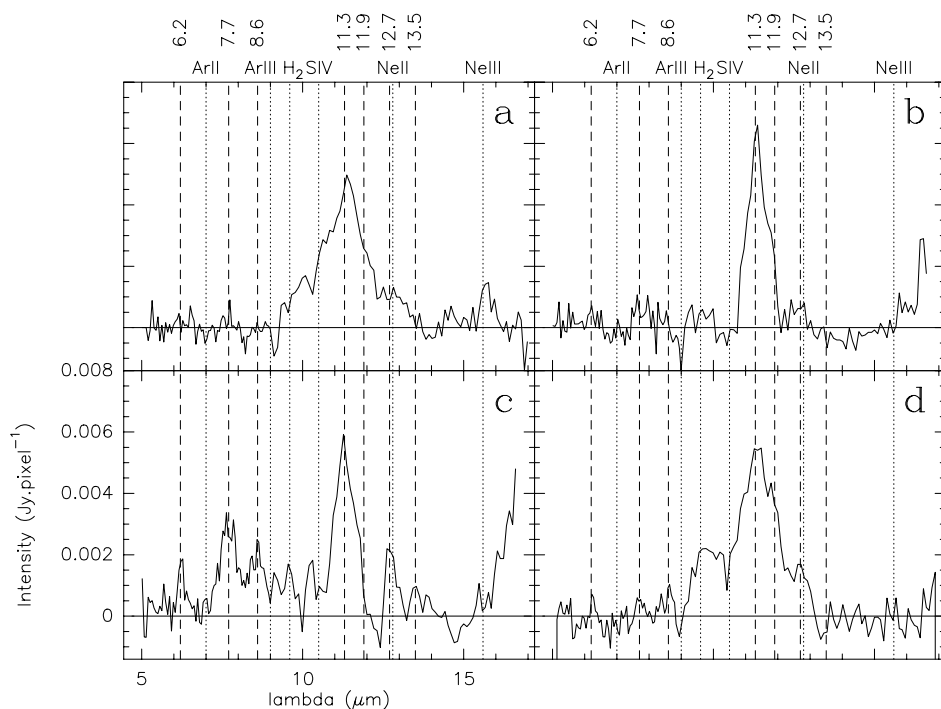


Fig. 3a–d. Differential mid-IR spectra of the 4 studied regions of M 31. **a:** center; **b:** bulge, 4.8′ North, 1.7′ West from the center; **c:** active region in the star-forming ring; **d:** quiet region in the star-forming ring. The long-wavelength parts of **b** and **c** are affected by the transient response of the detector. A first- or second-order baseline has been subtracted from the spectra, so that there is no information on the continuum. Lines of NeIII (**a**), 6.2, 7.7 and 8.6 μm UIB (**c**) are detected. NeII and/or the 12.7 μm UIB are also seen. Emission at 9 μm (H_2 ?) is visible, mostly in **d**. The flux scale uncertainty is 30%.

(resolution $23''$) at three positions in the studied region. These positions are plotted in Fig. 2.

It is not straightforward to draw conclusions from the comparison of these different tracers. But it is clear that the emission does not come from circumstellar envelopes, the stars having a very different distribution.

3.2. The mid-IR spectrum in the inner 3′ of M 31

Fig. 3a shows the differential spectrum between the bright and the weak regions at 11.3 μm in Fig. 2. It is dominated by a broad 11.3 μm UIB, while the usual 6.2, 7.7 and 8.6 μm UIBs are weak or absent. Such an interstellar UIB spectrum has never been seen before to our knowledge: the 7.7 μm band is generally stronger than the 11.3 μm one. There is some fine-structure line emission of Ne III at 15.6 μm , and perhaps of Ne II at 12.8 μm , obviously due to the ionized gas. H_2 S(3) emission is also possibly present (Fig. 1) but, because it also appears in the ‘off’ spectrum, the feature is weak in Fig. 3a.

3.3. The mid-IR spectrum in the bulge

We have also observed the mid-IR spectrum of a region located 4.8′ North, 1.7′ West from the center. The position error can reach $15''$ for this region as well as for the two following ones. This is a quiet area in the bulge with negligible UV radiation. The differential spectrum between the 11.3 μm -bright and the 11.3 μm -faint regions of the 3′ field is displayed in Fig. 3b. It is similar to the spectrum of the center (Fig. 3a) but the 11.3 μm band is narrower.

3.4. Two mid-IR spectra in the star-formation ring

Figs. 3c and 3d display differential mid-IR spectra in two regions of the star-forming ring at 10 kpc from the center of M 31. That of Fig. 3c is from an active region for which the $3' \times 3'$ field was centered at the position $X = -43.5'$, $Y = 9'$ (see Loinard et al. 1996b), and that of Fig. 3d from a quieter region dominated by molecular gas with the field center at $X = -38'$, $Y = 1.5'$. The spectrum of the active region is dominated by a rather narrow 11.3 μm UIB, but the UIB at 6.2, 7.7 and 8.6 μm are relatively strong. The ‘satellite’ features at 12.7 and 13.5 μm are seen in many UIB spectra, but there might be some contribution of the $[\text{Ne II}]$ line to the 12.7 μm UIB.

The spectrum of the quieter region (Fig. 3d) is similar to that of the bulge (Fig. 3a), with a broad 11.3 μm band. The S(3) rotation line of H_2 might contribute to this band and perhaps also the $[\text{Ne II}]$ line.

4. Discussion and conclusions

The UIB spectra of Fig. 3a, 3b, 3d and to a lesser extent of Fig. 3c are extremely different from any interstellar spectrum known to us. We have not seen a similar laboratory spectrum either.

The UIBs are usually attributed to PAHs or very small carbonaceous grains. Whatever their exact origin, the 11.3 μm band and its satellites at 12.7 and 13.5 μm correspond to out-of-plane bending modes of aromatic C–H, while the 8.6 μm band is due to in-plane bending modes of aromatic C–H and the 6.2 and 7.7 μm bands to vibrations of the skeleton itself. The particles which emit in M 31 spectra do not fit in this scheme.

A clue to this mystery might reside in the different illumination conditions in M 31. The disk and the bulge of this galaxy are dominated by old stars, the present star-formation rate being quite weak even in the star-forming ring at 10 kpc radius. At the center, the UV flux is also very weak compared with the visible and near-infrared emission by the bulge stars. In another paper (Lequeux et al. 1998) we give quantitative estimates of the intensity ratio $I_{\lambda}(200\text{ nm})/I_{\lambda}(550\text{ nm})$ in the studied regions of M 31. In the center and in the quiet field of the ring this ratio is $\simeq 0.03$ and it is even less in the bulge field. For comparison the same ratio is 0.6 in the Solar neighbourhood. Only in the star-forming regions of the ring is this ratio larger than near the Sun. It might then be that the energy of the red and near-IR photons is insufficient to heat through single-photon absorption the very small grains or PAHs responsible for the UIBs to temperatures $\simeq 200\text{ K}$. At such temperatures the $11.3\text{ }\mu\text{m}$ band would be excited, but not the bands near $8\text{ }\mu\text{m}$. However this hypothesis requires a fine-tuning of the properties of the UIB carriers which seems unlikely.

Alternatively, the UIB carriers might have different properties in the M 31 environments. We propose that what we see is the emission of amorphous hydrogenated carbon (HAC) particles as produced in the envelopes of carbon stars and not yet graphitized by UV heating. Ryter (1991) (see also Cherchneff et al. 1992) has given reasons why the usual UIB carriers (PAHs?), are not abundantly produced in these envelopes but that HACs are rather produced there. HAC particles are believed to contain microcrystals of graphite oriented randomly (Duley & Williams 1981). As discussed by them, they do not emit the 6.2 and $7.7\text{ }\mu\text{m}$ bands because the C-C ring vibrations are broadened to a continuum in the disordered solid. The active C-H bonds on the periphery of the grains produce stretching vibrations at 3.3 or $3.4\text{ }\mu\text{m}$ and out-of-plane aromatic bending vibrations at $11.3\text{ }\mu\text{m}$ (probably broadened by solid interaction). The in-plane C-H bending vibrations at $8.6\text{ }\mu\text{m}$ should be weak or absent due to disorder at the surface.

Examination of spectra of carbon stars or post-AGB stars before the planetary nebula stage (e.g. Y Tau in Aitken et al. 1979, or many stars in Justtanont et al. 1996 and Groenewegen et al. 1998) confirms these predictions. They exhibit a broad $11.3\text{ }\mu\text{m}$ emission or absorption band with a variable shape very similar to what we see in M 31, an absorption at $3.4\text{ }\mu\text{m}$, but nothing at $8.6\text{ }\mu\text{m}$ with however a few exceptions. A complete ISO spectrum of IRC +10216 (J. Cernicharo, private communication) shows a strong and broad $11.3\text{ }\mu\text{m}$ emission band, but nothing conspicuous in the $5\text{--}9\text{ }\mu\text{m}$ range. The $11.3\text{ }\mu\text{m}$ band is often attributed to SiC but the evidence for this is not strong. These spectra fit very well with the above idea.

UV radiation will heat these tiny particles and graphitize them, making them able to emit the whole set of UIBs. This occurs clearly in planetary nebulae, but only a fraction of carbon stars evolve into planetary nebulae. We propose that in most of M 31 the UV field is so faint that this processing has not taken place appreciably in the interstellar medium. Even in the ring, the fresh particles produced by AGB stars still dominate.

There is an interesting consequence. The fact that elliptical galaxies with dust show a “normal” UIB spectrum (L. Vigroux, private communication) is a confirmation that their ISM comes from recent cannibalism of S or Irr galaxies in which the particles have been previously processed by UV radiation. Conversely, the ISM in the center and the bulge of M31 cannot come from accretion and must have been produced locally.

We believe that our observations give another, very strong evidence of the continuous formation and destruction of the UIB carriers in the interstellar medium (Boulanger et al. 1990).

Acknowledgements. We thank the anonymous referee for interesting comments.

References

- Abergel A., Désert F.X., Miville-Deschênes M.A., et al., 1998, Aitken D.K., Roche P.F., Spencer P.M., Jones B. 1979, ApJ 223, 925
 Biviano A. et al. 1997, *Proc. First ISO Workshop on Analytical Spectroscopy*, ESA SP-419
 Boulanger F., Falgarone, E., Puget J.L., Helou G. 1990, ApJ 364, 136
 Boulesteix J., Georgelin Y.P., Lecoarer E., Marcellin M., Monnet G. 1987, A&A 178, 91
 Brinks E., Shane W.W. 1984, A&AS 55, 179
 Cesarsky C.J., Abergel A., Agnèsè P. et al. 1996a, A&A 315, L32
 Cesarsky D., Lequeux J., Abergel A., et al. 1996b, A&A 315, L309
 Cherchneff I., Barker J.R., Tielens A.G.G.M. 1992, ApJ 401, 269
 Duley W.W., Williams D.A. 1981, MNRAS 196, 269
 Groenewegen M.A.T., Whitelock P.A., Smith C.H., Kerschbaum F. 1998, MNRAS 293, 18
 Hodge P.W. 1980, *Atlas of the Andromeda Galaxy*, University of Washington Press, Seattle
 Johnson H.M., Hanna M.M. 1972, ApJ 174, L71
 Justtanont K., Barlow M.J., Skinner C.J., Roche P.F., Aitken D.K., Smith C.H. 1996, A&A 309, 612
 Lequeux J., Pagani L., Cesarsky D. et al. 1998, A&A, submitted
 Loinard L., Allen R.J., Lequeux J. 1995, A&A 301, 68
 Loinard L., Allen R.J., Lequeux J. 1996a, A&A 310, 93
 Loinard L., Dame T.M., Koper E., Lequeux J., Thaddeus P., Young J.S. 1996b, ApJ 469, L101
 Reach W.T., Abergel A., Boulanger F. et al. 1996, A&A 315, L381
 Ryter C. 1991, Annales de Physique 16, 507
 Starck J.L., Abergel A., Aussel H., et al. 1998, A&AS in press
 Xu C., Helou G. 1996, ApJ 456, 152